
Accurate and Fast Federated Learning via IID and Communication-Aware Grouping

Jin-woo Lee¹ Jaehoon Oh¹ Yooju Shin¹ Jae-Gil Lee¹ Se-Young Yoon¹

Abstract

Federated learning has emerged as a new paradigm of collaborative machine learning; however, it has also faced several challenges such as non-independent and identically distributed (IID) data and high communication cost. To this end, we propose a novel framework of *IID and communication-aware group federated learning* that simultaneously maximizes both accuracy and communication speed by grouping nodes based on data distributions and physical locations of the nodes. Furthermore, we provide a formal convergence analysis and an efficient optimization algorithm called *FedAvg-IC*. Experimental results show that, compared with the state-of-the-art algorithms, FedAvg-IC improved the test accuracy by up to 22.2% and simultaneously reduced the communication time to as small as 12%.

1. Introduction

Federated learning (Konečný et al., 2016a; McMahan et al., 2017) enables mobile devices to collaboratively learn a shared model while keeping all training data on the devices, thus avoiding transferring data to the cloud or central server. In this framework, a *local* model is updated using the data on each device, and all local updates are periodically aggregated to the *global* model; then, each local model is synchronized with the global model. Federated learning is attracting more attention, as indicated by the recent release of TensorFlow Federated (TFF) in March 2019 (Google, 2019). One of the main reasons for this recent boom in federated learning is that it does not compromise user privacy. However, there are several challenges despite federated learning’s growing popularity. McMa-

han et al. (2017) pointed out that federated learning has three unique properties: non-independent and identically distributed (IID), unbalanced, and massively-distributed. In this study, we tackle the challenges for the non-IID and massively-distributed properties as follows:

- **Non-IID Challenge:** Because each mobile device typically stores the data generated by a particular user, each local data distribution does *not* represent the global population distribution. This non-IID property definitely hinders the convergence of federated learning and degrades prediction accuracy.
- **Limited Communication Challenge:** Because several thousands of devices typically participate in federated learning, the training process is massively distributed, thus causing a huge burden on the backbone (wireless) network (Park et al., 2018).

To the best of our knowledge, no existing work has addressed both of the above challenges simultaneously. However, there have been active studies on each challenge. Notably, Lin et al. (2018) proposed a group-based learning algorithm, where the nodes (i.e., devices) are grouped into node groups; the local models are first aggregated to a *group* model, and the group models are then aggregated to the global model. While the group-based learning relieves the non-IID issue, it may cause high communication overheads especially if far-away nodes belong to the same node group. Wang et al. (2019) proposed a resource-constrained optimization algorithm to optimize the number of communication rounds but did not address the non-IID issue. In contrast, Zhao et al. (2018) proposed a data sharing strategy that distributes a small subset of global data to all nodes for resolving the non-IIDness, but the additional global communication cost is not seriously considered and it somewhat violates the philosophy of federated learning.

In this paper, we propose a novel framework of *IID and communication-aware group federated learning* to address both challenges. Here, nodes are grouped by the *IID and communication-aware grouping* principle to make the data distribution of each group closer to the global IID data distribution and to reduce node-to-group communication simultaneously. Fig. 1, where the data distributions are distinguished by their different shapes, illustrates the

*Equal contribution ¹Korea Advanced Institute of Science and Technology. Correspondence to: Jin-woo Lee <jin-woo.lee@kaist.ac.kr>.

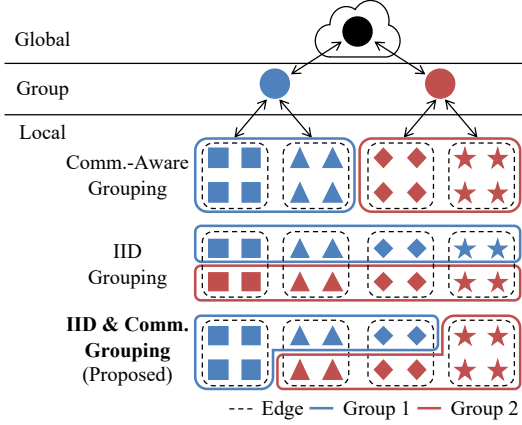


Figure 1: Concept of IID and communication-aware group federated learning.

proposed framework as well as two simple alternatives. Communication-aware grouping concentrates on the limited communication challenge at the cost of accuracy, and IID grouping concentrates on the non-IID challenge at the cost of efficiency. On the other hand, our proposed framework aims at presenting a *hybrid* of the two extreme cases. Overall, the key contributions are summarized as follows:

- **Problem Formulation** (Section 3): We formulate the problem as a bi-objective optimization that determines node groups by considering the difference in data distribution for the local-to-group and group-to-global levels as well as the communication delay based on the physical locations of nodes.
- **Convergence Analysis** (Section 4): We formally derive the convergence bound of group federated learning. As per our analysis, the optimal node grouping is achieved when the difference in data distribution for the group-to-global level and the group communication delay are simultaneously minimized.
- **Optimization Algorithm** (Section 5): We design a control algorithm, called *FedAvg-IC*, to find the near-optimal node grouping that minimizes both IID and communication costs.
- **High Performance** (Section 6): We empirically compared *FedAvg-IC* with three federated learning algorithms on four benchmark datasets. *FedAvg-IC* reached a higher accuracy by up to 22.2% and simultaneously reduced communication time to as small as 12%, compared with the three selected algorithms.

2. Preliminaries and Related Work

In this section, we first briefly describe *federated learning* and then survey relevant studies that handle either *non-IIDness* or *limited communication*.

2.1. Basics of Federated Learning

The objective of *federated learning* is to find an approximate solution of Eq. (1) (McMahan et al., 2017). Here, $F(\mathbf{w})$ is the loss of predictions with a model \mathbf{w} over the set of all data examples $\mathcal{D} \triangleq \cup_{i \in \mathcal{N}} \mathcal{D}_i$ across all nodes, where \mathcal{N} is the set of node indices, $F_i(\mathbf{w}) \triangleq \sum_{j \in \mathcal{D}_i} \frac{1}{|\mathcal{D}_i|} F_{ij}(\mathbf{w})$ is the loss of predictions with \mathbf{w} over the set of data examples \mathcal{D}_i on the i -th node, and $F_{ij}(\mathbf{w}) \triangleq l(\mathbf{w}, \mathbf{x}_{ij}, y_{ij})$ is the loss of a prediction with \mathbf{w} on the j -th data example $(\mathbf{x}_{ij}, y_{ij})$ on the i -th node.

$$\mathbf{w}^* \triangleq \arg \min_{\mathbf{w} \in \mathbb{R}^d} F(\mathbf{w}) \quad \text{where} \quad F(\mathbf{w}) \triangleq \sum_{i \in \mathcal{N}} \frac{|\mathcal{D}_i|}{|\mathcal{D}|} F_i(\mathbf{w}) \quad (1)$$

Federated Averaging (FedAvg) (McMahan et al., 2017), which is the canonical algorithm for federated learning in Eq. (1), involves *local update*, which learns a *local model* \mathbf{w}_i at the i -th node by performing gradient descent steps, and *global aggregation*, which learns the *global model* \mathbf{w} by aggregating all \mathbf{w}_i and synchronizes \mathbf{w}_i with \mathbf{w} every τ steps, as shown in Eq. (2).

$$\mathbf{w}_i(t) \triangleq \begin{cases} \mathbf{w}_i(t-1) - \eta \nabla F_i(\mathbf{w}_i(t-1)) & \text{if } t \bmod \tau \neq 0 \\ \mathbf{w}(t) & \text{if } t \bmod \tau = 0 \end{cases} \quad (2)$$

where $\mathbf{w}(t) \triangleq \sum_{i \in \mathcal{N}} \frac{|\mathcal{D}_i|}{|\mathcal{D}|} [\mathbf{w}_i(t-1) - \eta \nabla F_i(\mathbf{w}_i(t-1))]$

2.2. Related Work on the Non-IID Challenge

2.2.1. GROUP FEDERATED LEARNING

To reduce the learning divergence between \mathbf{w}_i and \mathbf{w} in Eq. (2), Lin et al. (2018) proposed a group-based architecture of allowing multiple intermediate aggregations before a global aggregation. Formally speaking, the set of all node indices \mathcal{N} is partitioned into sets of node indices for $|\mathcal{K}|$ *node groups* $\{\mathcal{N}^1, \mathcal{N}^2, \dots, \mathcal{N}^{|\mathcal{K}|}\}$, i.e., $\cup_{k \in \mathcal{K}} \mathcal{N}^k = \mathcal{N}$ and $\forall k \neq l, \mathcal{N}^k \cap \mathcal{N}^l = \emptyset$. Additionally, let \mathcal{D}^k be the set of data examples on the k -th node group and \mathcal{D}_i^k be its subset of \mathcal{D}^k on the i -th node. Then, the loss function of Eq. (1) is extended to that of Eq. (3) by considering the node groups.

$$F(\mathbf{w}) \triangleq \sum_{k \in \mathcal{K}} \frac{|\mathcal{D}^k|}{|\mathcal{D}|} F^k(\mathbf{w}), \quad F^k(\mathbf{w}) \triangleq \sum_{i \in \mathcal{N}^k} \frac{|\mathcal{D}_i^k|}{|\mathcal{D}^k|} F_i^k(\mathbf{w}) \quad (3)$$

Group federated learning was implemented as *hierarchical local SGD* (Lin et al., 2018), and it learns the *group model*

\mathbf{w}^k by aggregating all \mathbf{w}_i^k and synchronizes \mathbf{w}_i^k with \mathbf{w}^k every τ_1 steps, which can be expressed as Eq. (4).

$$\mathbf{w}_i^k(t) \triangleq \begin{cases} \mathbf{w}_i^k(t-1) - \eta \nabla F_i^k(\mathbf{w}_i^k(t-1)) & \text{if } t \bmod \tau_1 \neq 0 \\ \mathbf{w}^k(t) & \text{if } t \bmod \tau_1 = 0, \\ & t \bmod \tau_1 \tau_2 \neq 0 \\ \mathbf{w}(t) & \text{if } t \bmod \tau_1 \tau_2 = 0 \end{cases}$$

where $\mathbf{w}^k(t) \triangleq \sum_{i \in \mathcal{N}^k} \frac{|\mathcal{D}_i^k|}{|\mathcal{D}^k|} [\mathbf{w}_i^k(t-1) - \eta \nabla F_i^k(\mathbf{w}_i^k(t-1))]$

and $\mathbf{w}(t) \triangleq \sum_{k \in \mathcal{K}} \sum_{i \in \mathcal{N}^k} \frac{|\mathcal{D}_i^k|}{|\mathcal{D}|} [\mathbf{w}_i^k(t-1) - \eta \nabla F_i^k(\mathbf{w}_i^k(t-1))]$ (4)

2.2.2. GLOBAL-INFORMATION SHARING

Sharing global information is effective in mitigating the non-IIDness of a local node. The most common approach is to share a subset of global IID data samples to make the local data distribution closer to the population data distribution (Zhao et al., 2018; Yoshida et al., 2019). FSVRG (Konecný et al., 2016a) shares a subset of global data features to scale up the feature-related parameters of a local optimizer. FAug (Jeong et al., 2018) shares a generative model that can produce an augmented IID dataset.

2.3. Related Work on the Communication Challenge

2.3.1. COMMUNICATION-AWARE LEARNING

AdaptiveFL (Wang et al., 2019) extends FedAvg to adaptively optimize the number of global aggregations by considering resource consumption such as communication. FedCS (Nishio & Yonetani, 2019) minimizes the overall communication delay for a set of sampled learners by considering a round-trip time constraint. HierFAVG (Liu et al., 2019), which is the state-of-the-art approach for group federated learning, groups nodes by network edges to facilitate communication between the nodes in proximity. Similarly, we define a novel optimization problem that considers both IID and communication costs for maximizing accuracy and efficiency of federated learning, as shown in Section 3.

2.3.2. COMMUNICATION OVERHEAD REDUCTION

Reducing communication overheads in federated learning usually leads to saving both communication and computation resources. The overheads include the number of participating nodes and the amount of communication data. The participating nodes can be sampled by following a certain probability distribution (McMahan et al., 2017; Li et al., 2019; Sahu et al., 2018), but this approach is beyond the scope of this paper. Meanwhile, communication data size can be reduced by using a quantization or compression technique (Konecný et al., 2016b; Sattler et al., 2019) or by placing intermediate parameter servers in a network

topology (Bonawitz et al., 2019). We also attempt to reduce communication data size in Section 5.

Table 1: Summary of the notation.

Notation	Description
\mathbf{w}_i^k	Local model of i -th node in k -th group
\mathbf{w}^k	Group model of k -th group
$\mathbf{w}(T)$	Global model after T steps
τ_1	# of local updates per group aggregation
τ_2	# of group aggregations per global aggregation
$[r]$	Group interval, i.e., $[(r-1)\tau_1, r\tau_1]$
$[l]$	Global interval, i.e., $[(l-1)\tau_1\tau_2, l\tau_1\tau_2]$
δ	Local-to-group divergence
Δ	Group-to-global divergence

3. IID and Communication-Aware Group Federated Learning

Our primary goal is to train a global model that simultaneously minimizes the global loss in Eq. (3) and the total communication delay by considering the aforementioned challenges, which can be formulated as Eq. (5).

$$\min_{\tau_1, \tau_2, |\mathcal{K}|, \mathbf{z}} \{F(\mathbf{w}(T)), (d_{group}(\tau_2 - 1) + d_{global})\} \quad (5)$$

- The *IID objective* is defined as the minimization of global loss after T steps, and the *communication objective* is defined as the minimization of total communication delay, where d_{group} and d_{global} represent the communication delay (e.g., in seconds) spent for a single iteration of group and global aggregations, respectively. d_{group} and d_{global} can be easily estimated from a given network topology (e.g., by using hop counts (Vahdat & Becker, 2000)). $\tau_2 - 1$ implies that a global aggregation takes over a group aggregation every τ_2 steps.
- The optimization parameters are the learning steps τ_1 and τ_2 , the number of node groups $|\mathcal{K}|$, and the group membership $\mathbf{z} \triangleq (z_i | [\forall i \in \mathcal{N}, \exists k \in \mathcal{K}](z_i = k))$.

4. Theoretical Analysis

In this section, we provide a theoretical analysis of the IID and communication-aware group federated learning. Based on an assumption and definitions in Section 4.1, we analyze the convergence of group federated learning in Section 4.2 and draw notable remarks for the main problem in Section 4.3. Table 1 summarizes the notation used in this paper.

4.1. Assumption and Definitions

We make the following assumption for the loss function F_i^k , as in many other relevant studies (Liu et al., 2019; Wang et al., 2019). For every i and k , ① F_i^k is con-

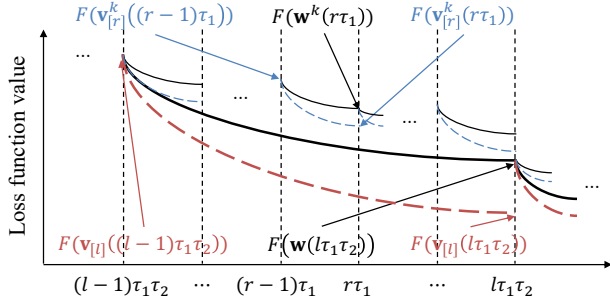


Figure 2: Illustration of loss divergence and synchronization between \mathbf{w}^k and $\mathbf{v}_{[r]}^k$ and between \mathbf{w} and $\mathbf{v}_{[l]}$.

vex¹; ② F_i^k is ρ -Lipschitz, i.e., $\|F_i^k(\mathbf{w}) - F_i^k(\mathbf{w}')\| \leq \rho\|\mathbf{w} - \mathbf{w}'\|$ for any \mathbf{w} and \mathbf{w}' ; and ③ F_i^k is β -smooth, i.e., $\|\nabla F_i^k(\mathbf{w}) - \nabla F_i^k(\mathbf{w}')\| \leq \beta\|\mathbf{w} - \mathbf{w}'\|$ for any \mathbf{w} and \mathbf{w}' .

Under this assumption, Lemma 1 holds for the group and global loss functions.

Lemma 1. F and F^k are convex, ρ -Lipschitz, and β -smooth.

Proof. It is straightforward from the aforementioned assumption and the definitions of F and F^k in Eq. (3). \square

We introduce two types of intervals depending on the learning level: a *group interval*, $[r] \triangleq [(r-1)\tau_1, r\tau_1]$, indicates an interval between two successive *group* aggregations, and a *global interval*, $[l] \triangleq [(l-1)\tau_1\tau_2, l\tau_1\tau_2]$, indicates an interval between two successive *global* aggregations.

Next, we introduce the notion of *group-based virtual learning* in Definition 1, where training data is assumed to exist on a *virtual* central repository for each model.

Definition 1 (Group-Based Virtual Learning). Given a certain group membership \mathbf{z} , for any k , $[r]$, and $[l]$, the *virtual group model* $\mathbf{v}_{[r]}^k$ and *virtual global model* $\mathbf{v}_{[l]}$ are updated by performing gradient descent steps on the centralized data examples for \mathcal{N}^k and \mathcal{N} , respectively, and synchronized with the federated group model \mathbf{w}^k and the global model \mathbf{w} at the beginning of each interval, as in Eq. (6).

$$\mathbf{v}_{[r]}^k(t) \triangleq \begin{cases} \mathbf{w}^k(t) & \text{if } t = (m-1)\tau_1, \\ \mathbf{v}_{[r]}^k(t-1) - \eta\nabla F^k(\mathbf{v}_{[r]}^k(t-1)) & \text{otherwise} \end{cases}$$

$$\mathbf{v}_{[l]}(t) \triangleq \begin{cases} \mathbf{w}(t) & \text{if } t = (n-1)\tau_1\tau_2, \\ \mathbf{v}_{[l]}(t-1) - \eta\nabla F(\mathbf{v}_{[l]}(t-1)) & \text{otherwise} \end{cases} \quad \square \quad (6)$$

To facilitate the interpretation, Fig. 2 shows how a virtual model \mathbf{v} is updated, following Definition 1. For example, $\mathbf{v}_{[l]}$ starts diverging from \mathbf{w} after $(l-1)\tau_1\tau_2$ and becomes synchronized with \mathbf{w} at $l\tau_1\tau_2$.

¹We will empirically show that a non-convex function works well in Section 6.

Then, we formalize *group-based gradient divergence* in Definition 2 that models the impact of the difference in data distributions across nodes on federated learning.

Definition 2 (Group-Based Gradient Divergence). Given a certain group membership \mathbf{z} , for any i , k , and \mathbf{w} , δ_i^k is defined as the gradient difference between the i -th local loss and the k -th group loss; Δ^k is defined as the gradient difference between the k -th group loss and the global loss, which can be expressed as Eq. (7).

$$\delta_i^k \triangleq \|\nabla F_i^k(\mathbf{w}) - \nabla F^k(\mathbf{w})\|,$$

$$\Delta^k \triangleq \|\nabla F^k(\mathbf{w}) - \nabla F(\mathbf{w})\| \quad (7)$$

Then, the *local-to-group divergence* δ and the *group-to-global divergence* Δ are formulated as Eq. (8).

$$\delta \triangleq \sum_{k \in \mathcal{K}} \sum_{i \in \mathcal{N}^k} \frac{|\mathcal{D}_i^k|}{|\mathcal{D}|} \delta_i^k, \quad \Delta \triangleq \sum_{k \in \mathcal{K}} \frac{|\mathcal{D}^k|}{|\mathcal{D}|} \Delta^k \quad \square \quad (8)$$

4.2. Convergence of the Group Federated Learning

We provide a proof sketch for the convergence of the global loss $F(\mathbf{w}(T))$ in Appendix A.1, which derives Theorem 1.

Theorem 1. Let $\omega \triangleq \min_q \frac{1}{\|\mathbf{v}_{[l]}((l-1)\tau_1\tau_2) - \mathbf{w}^*\|^2}$. When $\eta \leq \frac{1}{\beta}$, the convergence upper bound of group federated learning after T steps can be expressed as Eq. (9).

$$F(\mathbf{w}(T)) - F(\mathbf{w}^*) \leq \frac{1}{2\tau_1\tau_2\eta\omega}$$

$$+ \rho \left(\frac{\delta}{\beta} ((\eta\beta + 1)^{\tau_1} - 1) + \frac{\Delta}{\beta} ((\eta\beta + 1)^{\tau_1\tau_2} - 1) \right) \quad (9)$$

Proof. Please refer to Appendix A.3 for details. \square

From Eq. (9), it is straightforward to see that the optimality gap is dominantly affected by τ_1 , τ_2 , δ , and Δ . Therefore, given small values, the convergence is guaranteed.

4.3. Theoretical Analysis for the Main Problem

Based on the convergence analysis, we interpret the IID and communication-aware group federated learning as follows.

Remark 1 (Dominance of Δ). The IID objective ($\min F(\mathbf{w}(T))$) in Eq. (5) is the same as minimizing $F(\mathbf{w}(T)) - F(\mathbf{w}^*)$ in Eq. (9) because $F(\mathbf{w}^*)$ is a constant. Thus, given τ_1 , τ_2 , and $|\mathcal{K}|$, because Δ is the most dominant factor in Eq. (9), it is important for the IID objective to reduce Δ by changing \mathbf{z} .

Remark 2 (Dominance of d_{group}). For the communication objective ($\min d_{group}(\tau_2 - 1) + d_{global}$), because d_{global} is not affected by a certain node grouping from the definition of global aggregation in Eq. (4), given τ_1 , τ_2 , and $|\mathcal{K}|$, it is important for the communication objective to reduce d_{group} by changing \mathbf{z} .

In conclusion, we establish the **IID and communication-aware grouping** principle: a group federated learning algorithm should group nodes by simultaneously minimizing Δ and d_{group} to maximize both accuracy and efficiency.

5. Optimization Algorithm: FedAvg-IC

To solve Eq. (5), an efficient heuristic algorithm is essential because the grouping problem itself is NP-Hard with the complexity of $O(|\mathcal{N}|^{|\mathcal{K}|})$. In this regard, we propose a novel algorithm called **FedAvg-IC** (*Federated Averaging with IID and Communication-Aware Grouping*).

5.1. Algorithm Description

FedAvg-IC aims at quickly finding an accurate global model based on the near-optimal node grouping that follows the IID and communication-aware grouping principle, for which we adopt the *k-medoids* algorithm (Park & Jun, 2009). The node grouping involves assigning each node to the closest medoid node and updating a representative medoid node for each group. Here, the distance is measured by the cost functions defined as follows.

Assign Cost: To evaluate the cost of assigning the i -th node to the k -th group, we model the IID cost ($\text{COST}_{A,iid}$) and communication cost ($\text{COST}_{A,comm}$) using Δ^k in Eq. (7) and the hop distance between the i -th node and i_k -th medoid node, respectively, as shown in Eq. (10).

$$\begin{aligned} \text{COST}_{A,iid}(i, k) &\triangleq \Delta^k \text{ where } i \in \mathcal{N}^k \\ \text{COST}_{A,comm}(i, k) &\triangleq \text{HOPDISTANCE}(i, i_k) \end{aligned} \quad (10)$$

Update Cost: To evaluate the cost of selecting the i -th node in the k -th group as a new medoid for the group, we model the IID cost ($\text{COST}_{U,iid}$) and the communication cost ($\text{COST}_{U,comm}$) by the local-to-global divergence of the i -th node and the sum of hop distances to all other nodes in the group, respectively, as shown in Eq. (11).

$$\begin{aligned} \text{COST}_{U,iid}(i, k) &\triangleq \frac{|\mathcal{D}_i^k|}{|\mathcal{D}|} \|\nabla F_i^k(\mathbf{w}) - \nabla F(\mathbf{w})\| \\ \text{COST}_{U,comm}(i, k) &\triangleq \sum_{j \in \mathcal{N}^k} \text{HOPDISTANCE}(i, j) \end{aligned} \quad (11)$$

Combined Cost: Given $X \in \{A, U\}$, $\text{COST}_{X,iid}$ (IID cost) and $\text{COST}_{X,comm}$ (communication cost) are combined into a single cost, as shown in Eq. (12).

$$\text{COST}_X \triangleq \alpha_{iid} \frac{\text{COST}_{X,iid}}{C_{X,iid}} + \alpha_{comm} \frac{\text{COST}_{X,comm}}{C_{X,comm}} \quad (12)$$

α is the weight, and C is the normalizing constant².

Algorithm 1 shows the overall procedure of FedAvg-IC. It takes the set of node indices \mathcal{N} , the final time T , the learning steps τ_1^0 and τ_2^0 , and the number of node groups $|\mathcal{K}|$

² C is set to be the first cost value in the optimization process (Grodzевич & Romanko, 2006).

³ $[X]_i$ denotes the variable reference of X at a node i .

Algorithm 1 FedAvg-IC

INPUT: $\mathcal{N}, T, \tau_1^0, \tau_2^0, |\mathcal{K}|$
 OUTPUT: $\mathbf{w}(T)$

- 1: Initialize $\mathbf{w}(0)$ and \mathbf{z} randomly, $\tau_1 \leftarrow 1, \tau_2 \leftarrow 1$
- 2: $[\mathbf{w}_i^k(0)]_{i \in \mathcal{N}} \leftarrow \mathbf{w}(0)$ /* Initial global broadcast³*/
- 3: **for** $t \leftarrow 1, 2, \dots, T$ **do**
- 4: **for each** $i \in \mathcal{N}$ **in parallel do** /* Local */
- 5: $\mathbf{w}_i^k(t) \leftarrow \mathbf{w}_i^k(t-1) - \eta \nabla F_i^k(\mathbf{w}_i^k(t-1))$
- 6: **if** $(t-1) \bmod \tau_1 \tau_2 \neq 0$ **then** /* Group */
- 7: **for each** $k \in \mathcal{K}$ **in parallel do**
- 8: $[\mathbf{w}^k]_{i_k} \leftarrow \sum_{i \in \mathcal{N}^k} \frac{|\mathcal{D}_i^k|}{|\mathcal{D}^k|} [\mathbf{w}_i^k(t)]_i$
- 9: $[\mathbf{w}_i^k(t)]_{i \in \mathcal{N}^k} \leftarrow [\mathbf{w}^k]_{i_k}$
- 10: **if** $(t-1) \bmod \tau_1 \tau_2 = 0$ **then** /* Global */
- 11: $\mathbf{w} \leftarrow \sum_{i \in \mathcal{N}} \frac{|\mathcal{D}_i^k|}{|\mathcal{D}|} [\mathbf{w}_i^k(t)]_i$
- 12: $[\mathbf{w}_i^k(t)]_{i \in \mathcal{N}} \leftarrow \mathbf{w}$
- 13: **if** \mathcal{N} is not grouped **then**
- 14: $\mathbf{z} \leftarrow \text{NODE_GROUPING}(\mathbf{z})$
- 15: $(\tau_1, \tau_2) \leftarrow (\tau_1^0, \tau_2^0)$
- 16: **function** $\text{NODE_GROUPING}(\mathbf{z})$
- 17: Select random medoid nodes \mathcal{N}_m
- 18: $\mathbf{z} \leftarrow (\arg \min_{k \in \mathcal{K}} \text{COST}_A(i, k) | \forall i \in \mathcal{N})$
- 19: **until** the last COST_A is steady **do**
- 20: $\mathcal{N}_m \leftarrow (\arg \min_{i \in \mathcal{N}^k} \text{COST}_U(i, k) | \forall k \in \mathcal{K})$
- 21: $\mathbf{z} \leftarrow (\arg \min_{k \in \mathcal{K}} \text{COST}_A(i, k) | \forall i \in \mathcal{N})$
- 22: **return** \mathbf{z}

as the input and returns the final global model $\mathbf{w}(T)$ as the output. It begins by initializing the global model and group membership randomly (Line 1). Then, the global model is broadcast to all nodes (Line 2). Then, the local update is performed at each node (Lines 4–5); each group model is learned by aggregating all local models in the group and then broadcast back to all nodes (Lines 6–9); the global model is learned by aggregating all local models and then broadcast back to all nodes (Lines 10–12). After the first global aggregation, the group membership \mathbf{z} is updated (Line 14). Overall, Lines 3–15 repeat for T steps.

The NODE_GROUPING function attempts to find a group membership \mathbf{z} that reduces the combined cost in Eq. (12) to the extent possible. For this purpose, it begins by selecting random medoid nodes \mathcal{N}_m of size $|\mathcal{K}|$. Then, it iteratively updates \mathbf{z} by minimizing COST_A in Eq. (10) for all nodes and COST_U in Eq. (11) for all groups until the cost is steady (Lines 19–21).

6. Evaluation

6.1. Experimental Setting

Configuration: We developed a federated learning simulator to extensively evaluate the performance of various algorithms, models, datasets, and networks based on TensorFlow 1.14.0. Please refer to Appendix C.1 for details.

Algorithms: We compared the following *three* algorithms.

- **FedAvg** (McMahan et al., 2017), which is used as a baseline, does not consider node grouping at all.
- **HierFAVG** (Liu et al., 2019) groups nodes by network edges to facilitate communication between nodes.
- **FedAvg-IC** groups nodes by minimizing both IID and communication costs. We also considered FedAvg-IC that only minimizes either IID or communication cost as FedAvg-I or FedAvg-C, respectively.

Datasets: We used *four* datasets, ① MNIST-O (LeCun et al., 1998), ② MNIST-F (Xiao et al., 2017), ③ FEMNIST (Caldas et al., 2018), and ④ CelebA (Liu et al., 2015), which consist of 70,000, 70,000, 78,353, and 10,014 examples, respectively. The ratio of train/validation/test examples was 3:1:1, as suggested by Caldas et al. (2018).

Table 2: Class diversity across nodes and edges. An entry is the number of classes per node or edge.

	<i>Dtt</i>	<i>Dtq</i>	<i>Dth</i>	<i>Dqq</i>	<i>Dqh</i>	<i>Dhh</i>
Node	<i>tenth</i>	<i>tenth</i>	<i>tenth</i>	<i>quarter</i>	<i>quarter</i>	<i>half</i>
Edge	<i>tenth</i>	<i>quarter</i>	<i>half</i>	<i>quarter</i>	<i>half</i>	<i>half</i>

Data Distribution: To simulate a wide range of non-IIDness, we designed *six* cases of class diversity on each node and edge, as shown in Table 2. For example, in the *Dtq* setting, only a tenth of the classes can exist per node, and a quarter of the classes can exist per edge.

Models: We used *three* training models, ① the softmax regression (SR), ② the 2 layered perceptron neural network (2NN), and ③ the convolutional neural network (CNN). Please refer to Appendix C.1 for details.

Methodology: Deterministic gradient descent (DGD) was used for the SR to solve convex problems, and stochastic gradient descent (SGD) was used for the 2NN and the CNN to solve non-convex problems. We evaluate each algorithm five times and report the average with standard deviation.

6.2. Accuracy Results

Fig. 3 and Fig. 4a show the test accuracy of three federated learning algorithms on a non-IID (*Dtt*) dataset according to the elapsed time and epoch, respectively. Overall, FedAvg-IC outperformed FedAvg by up to 17.4% (Fig. 3d) and HierFAVG by up to 22.2% (Fig. 3b). In Fig. 4a, the algo-

gorithms that considered communication such as FedAvg-IC and FedAvg-C outperformed the others. The higher accuracy of FedAvg-IC is attributed to a decreased Δ in the IID cost in Eq. (12). Please refer to Appendix C.2 for details.

6.3. Efficiency Results

Table 3: Elapsed time (in seconds) of the algorithms on the non-IID and IID datasets at the final test accuracy of the baseline FedAvg within a given time, where the final accuracy is specified in parenthesis next to each model name.

	Non-IID (<i>Dtt</i>)		
	SR(84%)	2NN(73%)	CNN(83%)
FedAvg	50	300	300
HierFAVG	29(1.7x)	–	–
FedAvg-IC	6(8.3x)	47(6.4x)	149(2.0x)
	IID (<i>Dhh</i>)		
	SR(86%)	2NN(90%)	CNN(96%)
FedAvg	100	600	600
HierFAVG	29(3.4x)	468(1.3x)	–
FedAvg-IC	18(5.6x)	291(2.1x)	543(1.1x)

Table 3 shows the elapsed time and speedup on the most non-IID (*Dtt*) and IID (*Dhh*) datasets. In terms of the elapsed time, FedAvg-IC outperformed FedAvg and HierFAVG by up to 8.3 times and 4.8 times, respectively. Even though HierFAVG is in favor of communication efficiency, because the edge-based learning of HierFAVG degrades the accuracy in non-IID settings, it did not reach the target accuracy for the 2NN and the CNN. The faster convergence speed of FedAvg-IC is attributed to a decreased d_{group} in Eq. (12) as well as a decreased communication data size by the combined aggregation. Please refer to Appendix C.2.

7. Conclusion

In this paper, we proposed a novel framework of *IID and communication-aware group federated learning* to address both the non-IID and limited communication challenges simultaneously. Our formal convergence analysis led to the IID and communication-aware grouping principle that is incorporated into our optimization algorithm *FedAvg-IC*. Extensive experiments were performed using our own federated learning simulator, and the results demonstrated that FedAvg-IC outperformed HierFAVG by up to 22.2% in terms of test accuracy and FedAvg by up to 8.3 times in terms of convergence speed. Overall, we believe that our framework has made important steps towards accurate and fast federated learning.

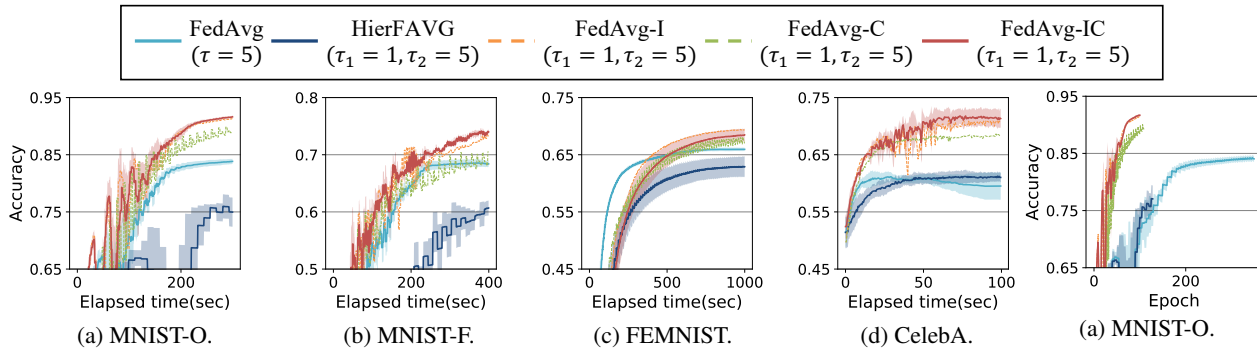


Figure 3: Test accuracy of the CNN on four datasets with D_{tt} according to elapsed time.

Figure 4: Test accuracy according to epochs.

References

Bonawitz, K., Eichner, H., Grieskamp, W., Huba, D., Ingerman, A., Ivanov, V., Kiddon, C., Konecny, J., Mazzocchi, S., McMahan, H. B., et al. Towards federated learning at scale: System design. In *Proc. 2nd Conf. on Systems and Machine Learning*, 2019.

Caldas, S., Duddu, S. M. K., Wu, P., Li, T., Konecny, J., McMahan, H. B., Smith, V., and Talwalkar, A. Leaf: A benchmark for federated settings. *arXiv:1812.01097*, 2018.

Cisco. Cisco annual internet report, 2018–2023, 2020.

Dean, J. and Ghemawat, S. MapReduce: simplified data processing on large clusters. *Communications of the ACM*, 51(1):107–113, 2008.

Google. TensorFlow Federated. https://www.tensorflow.org/federated/federated_learning, 2019. Accessed: 2020-06-08.

Grodzевич, O. and Romanko, O. Normalization and other topics in multi-objective optimization. In *Proc. Fields–MITACS Industrial Problems Workshop*, 2006.

Isard, M., Budiу, M., Yu, Y., Birrell, A., and Fetterly, D. Dryad: distributed data-parallel programs from sequential building blocks. *ACM SIGOPS Operating Systems Review*, 41(3):59–72, 2007.

Jeong, E., Oh, S., Kim, H., Park, J., Bennis, M., and Kim, S.-L. Communication-efficient on-device machine learning: Federated distillation and augmentation under non-iid private data. *arXiv:1811.11479*, 2018.

Konecny, J., McMahan, H. B., Ramage, D., and Richtárik, P. Federated optimization: Distributed machine learning for on-device intelligence. *arXiv:1610.02527*, 2016a.

Konecny, J., McMahan, H. B., Yu, F. X., Richtárik, P., Suresh, A. T., and Bacon, D. Federated learning: Strategies for improving communication efficiency. In *Proc.*

NIPS 2016 Workshop on Private Multi-Party Machine Learning, 2016b.

LeCun, Y., Bottou, L., Bengio, Y., Haffner, P., et al. Gradient-based learning applied to document recognition. *Proc. IEEE*, 86(11):2278–2324, 1998.

Li, X., Huang, K., Yang, W., Wang, S., and Zhang, Z. On the convergence of fedavg on non-iid data. *arXiv:1907.02189*, 2019.

Lin, T., Stich, S. U., Patel, K. K., and Jaggi, M. Don’t use large mini-batches, use local sgd. *arXiv:1808.07217*, 2018.

Liu, L., Zhang, J., Song, S., and Letaief, K. B. Edge-assisted hierarchical federated learning with non-iid data. *arXiv:1905.06641*, 2019.

Liu, Z., Luo, P., Wang, X., and Tang, X. Deep learning face attributes in the wild. In *Proc. 2015 Int’l Conf. on Computer Vision (ICCV)*, December 2015.

McMahan, H. B., Moore, E., Ramage, D., Hampson, S., et al. Communication-efficient learning of deep networks from decentralized data. In *Proc. 20th Int’l Conf. Artificial Intelligence and Statistics (AISTATS)*, pp. 1273–1282, 2017.

Nishio, T. and Yonetani, R. Client selection for federated learning with heterogeneous resources in mobile edge. In *Proc. IEEE Int’l Conf. on Communications*, pp. 1–7, 2019.

Park, H.-S. and Jun, C.-H. A simple and fast algorithm for k-medoids clustering. *Expert Systems with Applications*, 36(2):3336–3341, 2009.

Park, J., Samarakoon, S., Bennis, M., and Debbah, M. Wireless network intelligence at the edge. *arXiv:1812.02858*, 2018.

Sahu, A. K., Li, T., Sanjabi, M., Zaheer, M., Talwalkar, A., and Smith, V. On the convergence of federated optimization in heterogeneous networks. *arXiv:1812.06127*, 2018.

Sattler, F., Wiedemann, S., Müller, K.-R., and Samek, W. Robust and communication-efficient federated learning from non-iid data. *arXiv:1903.02891*, 2019.

Singla, A., Hong, C.-Y., Popa, L., and Godfrey, P. B. Jellyfish: Networking data centers randomly. In *9th USENIX Symposium on Networked Systems Design and Implementation (NSDI)*, pp. 225–238, 2012.

Vahdat, A. and Becker, D. Epidemic routing for partially-connected ad hoc networks. Technical report, Duke University, 2000.

Wang, S., Tuor, T., Salonidis, T., Leung, K. K., Makaya, C., He, T., and Chan, K. Adaptive federated learning in resource constrained edge computing systems. *IEEE Journal on Selected Areas in Communications*, 37(6):1205–1221, 2019.

Xiao, H., Rasul, K., and Vollgraf, R. Fashion-mnist: a novel image dataset for benchmarking machine learning algorithms. *arXiv:1708.07747*, 2017.

Yoshida, N., Nishio, T., Morikura, M., Yamamoto, K., and Yonetani, R. Hybrid-FL: Cooperative learning mechanism using non-iid data in wireless networks. *arXiv:1905.07210*, 2019.

Zhao, Y., Li, M., Lai, L., Suda, N., Civin, D., and Chandra, V. Federated learning with non-iid data. *arXiv:1806.00582*, 2018.

A. Convergence of the Group Federated Learning

A.1. Proof Sketch

We sketch the proof for the convergence of the global loss $F(\mathbf{w}(T))$ in Eq. (3) through the following three steps.

- **Step 1** (Local Learning Divergence): For a *group* interval $[r]$, we find the loss divergence between a local model and a virtual group model, $F(\mathbf{w}_i^k(t)) - F(\mathbf{v}_{[r]}^k(t))$.
- **Step 2** (Group Learning Divergence): For a *global* interval $[l]$, we find the loss divergence between a virtual group model and a virtual global model, $F(\mathbf{v}_{[r]}^k(t)) - F(\mathbf{v}_{[l]}(t))$. Then, by combining the aforementioned two loss divergences for all local models \mathbf{w}_i^k , we obtain the loss divergence between a federated global model and a virtual global model, $F(\mathbf{w}(t)) - F(\mathbf{v}_{[l]}(t))$.

- **Step 3** (Global Learning Divergence): For *all* global intervals, by combining $F(\mathbf{w}(t)) - F(\mathbf{v}_{[l]}(t))$ from Step 2 with the loss divergence between a virtual global model and the optimal model, $F(\mathbf{v}_{[l]}(t)) - F(\mathbf{w}^*)$, we finally obtain $F(\mathbf{w}(T)) - F(\mathbf{w}^*)$.

Corresponding to Steps 1 and 2 of the proof sketch, Lemma 2 gives an upper bound between a federated global model $\mathbf{w}(t)$ and a virtual global model $\mathbf{v}_{[l]}(t)$.

Lemma 2. For any global interval $[l]$ and $t \in [l]$, if F_i^k is β -smooth for every i and k in Eq. (7), then Eq. (13) holds.

$$\begin{aligned} & \|\mathbf{w}(t) - \mathbf{v}_{[l]}(t)\| \\ & \leq \frac{\delta}{\beta} ((\eta\beta + 1)^{\tau_1} - 1) + \frac{\Delta}{\beta} ((\eta\beta + 1)^{\tau_1\tau_2} - 1) \end{aligned} \quad (13)$$

Proof. Please refer to Appendix A.2 for details. \square

Finally, corresponding to Step 3 of the proof sketch, Theorem 1 is derived from Lemma 2.

A.2. Proof of Lemma 2

To prove Lemma 2, we introduce an auxiliary lemma (Lemma 3).

Lemma 3. For any $[r]$, $[l]$, and $t \in [(r-1)\tau_1, r\tau_1] \subset [(l-1)\tau_1\tau_2, l\tau_1\tau_2]$, an upper bound of the norm of the difference between a local model and the virtual global model can be expressed as Eq. (14).

$$\begin{aligned} & \|\mathbf{w}_i^k(t) - \mathbf{v}_{[l]}(t)\| \\ & \leq \frac{\delta_i^k}{\beta} ((\eta\beta + 1)^{t-(r-1)\tau_1} - 1) + \frac{\Delta^k}{\beta} ((\eta\beta + 1)^{t-(l-1)\tau_1\tau_2} - 1) \end{aligned} \quad (14)$$

Proof. From the triangle inequality, one can simply derive Eq. (15).

$$\begin{aligned} & \|\mathbf{w}_i^k(t) - \mathbf{v}_{[l]}(t)\| \\ & = \left\| \mathbf{w}_i^k(t) - \mathbf{v}_{[r]}^k(t) + \mathbf{v}_{[r]}^k(t) - \mathbf{v}_{[l]}(t) \right\| \\ & \leq \left\| \mathbf{w}_i^k(t) - \mathbf{v}_{[r]}^k(t) \right\| + \left\| \mathbf{v}_{[r]}^k(t) - \mathbf{v}_{[l]}(t) \right\| \end{aligned} \quad (15)$$

To conclude this proof, it thus suffices to show Eq. (16) and (17).

$$\left\| \mathbf{w}_i^k(t) - \mathbf{v}_{[r]}^k(t) \right\| \leq \frac{\delta_i^k}{\beta} ((\eta\beta + 1)^{t-(r-1)\tau_1} - 1) \quad (16)$$

$$\left\| \mathbf{v}_{[r]}^k(t) - \mathbf{v}_{[l]}(t) \right\| \leq \frac{\Delta^k}{\beta} ((\eta\beta + 1)^{t-(l-1)\tau_1\tau_2} - 1) \quad (17)$$

Then, by putting Eq. (16) and (17) into Eq. (15), we can confirm Lemma 3.

Both Eq. (16) and (17) can be easily drawn from the β -smooth property of F_i^k and F^k . From Eq. (4) and (6), we can derive Eq. (18).

$$\begin{aligned}
 & \left\| \mathbf{w}_i^k(t) - \mathbf{v}_{[r]}^k(t) \right\| \\
 &= \left\| \mathbf{w}_i^k(t-1) - \eta \nabla F_i^k(\mathbf{w}_i^k(t-1)) \right. \\
 & \quad \left. - \mathbf{v}_{[r]}^k(t-1) + \eta \nabla F^k(\mathbf{v}_{[r]}^k(t-1)) \right\| \\
 &\leq \left\| \mathbf{w}_i^k(t-1) - \mathbf{v}_{[r]}^k(t-1) \right\| \\
 & \quad + \eta \left\| \nabla F_i^k(\mathbf{w}_i^k(t-1)) - \nabla F_i^k(\mathbf{v}_{[r]}^k(t-1)) \right\| \\
 & \quad + \eta \left\| \nabla F_i^k(\mathbf{v}_{[r]}^k(t-1)) - \nabla F^k(\mathbf{v}_{[r]}^k(t-1)) \right\| \\
 &\leq (\eta\beta + 1) \left\| \mathbf{w}_i^k(t-1) - \mathbf{v}_{[r]}^k(t-1) \right\| + \eta\delta_i^k
 \end{aligned} \tag{18}$$

The last inequality stems from the β -smoothness of F_i^k and Definition 2.

Then, since $\mathbf{w}_i^k(t) = \mathbf{w}^k(t) = \mathbf{v}_{[r]}^k(t)$ at every group aggregation from Eq. (4) and (6), Eq. (18) can be rewritten as Eq. (19).

$$\begin{aligned}
 \left\| \mathbf{w}_i^k(t) - \mathbf{v}_{[r]}^k(t) \right\| &\leq \eta\delta_i^k \sum_{y=1}^{t-(r-1)\tau_1} (\eta\beta + 1)^{y-1} \\
 &= \frac{\delta_i^k}{\beta} \left((\eta\beta + 1)^{t-(r-1)\tau_1} - 1 \right)
 \end{aligned} \tag{19}$$

Analogously, one can derive Eq. (17). This is the end of the proof of Lemma 3. \square

For all t and q , from Lemma 3 and Jensen's inequality, Lemma 2 can be proven as in Eq. (20).

$$\begin{aligned}
 & \left\| \mathbf{w}(t) - \mathbf{v}_{[l]}(t) \right\| \\
 &\leq \sum_{k \in \mathcal{K}} \sum_{i \in \mathcal{N}^k} \frac{|\mathcal{D}_i^k|}{|\mathcal{D}|} \left\| \mathbf{w}_i^k(t) - \mathbf{v}_{[l]}(t) \right\| \\
 &\leq \frac{\delta}{\beta} \left((\eta\beta + 1)^{\tau_1} - 1 \right) + \frac{\Delta}{\beta} \left((\eta\beta + 1)^{\tau_1\tau_2} - 1 \right)
 \end{aligned} \tag{20}$$

Furthermore, since F is ρ -Lipschitz, Eq. (21) holds.

$$\begin{aligned}
 & F(\mathbf{w}(t)) - F(\mathbf{v}_{[l]}(t)) \\
 &\leq \rho \left(\frac{\delta}{\beta} \left((\eta\beta + 1)^{\tau_1} - 1 \right) + \frac{\Delta}{\beta} \left((\eta\beta + 1)^{\tau_1\tau_2} - 1 \right) \right)
 \end{aligned} \tag{21}$$

A.3. Proof of Theorem 1

Consider a certain learning step t in a l -th global interval, i.e., $t \in [(l-1)\tau_1\tau_2, l\tau_1\tau_2)$. Recall that $\mathbf{v}_{[l]}(t+1) =$

$\mathbf{v}_{[l]}(t) - \eta \nabla F(\mathbf{v}_{[l]}(t))$ from Eq. (6) in Section 4.1. Since F is convex, an upper bound of the loss divergence between the virtual global model and the optimal global model can be expressed as Eq. (22).

$$\begin{aligned}
 & F(\mathbf{v}_{[l]}(t)) - F(\mathbf{w}^*) \\
 &\leq \nabla F(\mathbf{v}_{[l]}(t))^\top (\mathbf{v}_{[l]}(t) - \mathbf{w}^*) \\
 &= \frac{1}{\eta} (\mathbf{v}_{[l]}(t) - \mathbf{v}_{[l]}(t+1))^\top (\mathbf{v}_{[l]}(t) - \mathbf{w}^*) \\
 &= \frac{1}{2\eta} \left(\|\mathbf{v}_{[l]}(t) - \mathbf{v}_{[l]}(t+1)\|^2 \right. \\
 & \quad \left. + \|\mathbf{v}_{[l]}(t) - \mathbf{w}^*\|^2 - \|\mathbf{v}_{[l]}(t+1) - \mathbf{w}^*\|^2 \right) \\
 &= \frac{\eta}{2} \|\nabla F(\mathbf{v}_{[l]}(t))\|^2 \\
 & \quad + \frac{1}{2\eta} \left(\|\mathbf{v}_{[l]}(t) - \mathbf{w}^*\|^2 - \|\mathbf{v}_{[l]}(t+1) - \mathbf{w}^*\|^2 \right)
 \end{aligned} \tag{22}$$

Additionally, since F is convex and β -smooth, when $\eta \leq \frac{1}{\beta}$, one can derive Eq. (23).

$$\begin{aligned}
 & F(\mathbf{v}_{[l]}(t)) - F(\mathbf{v}_{[l]}(t+1)) \\
 &\geq \nabla F(\mathbf{v}_{[l]}(t))^\top (\mathbf{v}_{[l]}(t) - \mathbf{v}_{[l]}(t+1)) \\
 & \quad - \frac{\beta}{2} \|\mathbf{v}_{[l]}(t) - \mathbf{v}_{[l]}(t+1)\|^2 \\
 &= \eta \|\nabla F(\mathbf{v}_{[l]}(t))\|^2 - \frac{\beta\eta^2}{2} \|\nabla F(\mathbf{v}_{[l]}(t))\|^2 \\
 &\geq \frac{\eta}{2} \|\nabla F(\mathbf{v}_{[l]}(t))\|^2
 \end{aligned} \tag{23}$$

From Eq. (22) and (23), Eq. (24) is derived by straightforward mathematics.

$$\begin{aligned}
 & F(\mathbf{v}_{[l]}(n\tau_1\tau_2)) - F(\mathbf{w}^*) \\
 &\leq \frac{1}{2\tau_1\tau_2\eta} \left(\|\mathbf{v}_{[l]}((l-1)\tau_1\tau_2) - \mathbf{w}^*\|^2 \right. \\
 & \quad \left. - \|\mathbf{v}_{[l]}(n\tau_1\tau_2) - \mathbf{w}^*\|^2 \right) \\
 &\leq \frac{1}{2\tau_1\tau_2\eta\omega}
 \end{aligned} \tag{24}$$

From Eq. (24) and Lemma 2, Theorem 1 can be proven as in Eq. (25).

$$\begin{aligned}
 & F(\mathbf{w}(T)) - F(\mathbf{w}^*) \leq \frac{1}{2\tau_1\tau_2\eta\omega} \\
 & \quad + \rho \left(\frac{\delta}{\beta} \left((\eta\beta + 1)^{\tau_1} - 1 \right) + \frac{\Delta}{\beta} \left((\eta\beta + 1)^{\tau_1\tau_2} - 1 \right) \right)
 \end{aligned} \tag{25}$$

B. Advanced Implementation Technique

In addition, we propose a novel *combined aggregation* technique that reduces the size of communication data in FedAvg-IC. Fig. 5 represents an example of the combined

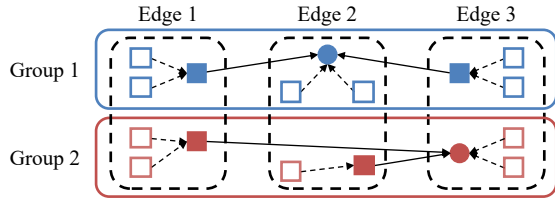


Figure 5: An example of combined aggregation.

aggregation. It is obvious that communication cost is almost negligible within an edge, and a group may consist of a few edges. Then, a certain local aggregation server (solid squares) can locally aggregate (dashed arrows) local models (hollow squares) in the same edge and send (solid arrows) the locally aggregated model to the group or global aggregation server (solid circles) with reduced communication data. This technique can be applied to both group and global aggregations as well as both group and global broadcasts inversely. We also note that this technique is similar to the partial aggregation of Dryad (Isard et al., 2007) and the combiner of MapReduce (Dean & Ghemawat, 2008).

C. Supplementary Evaluation Material

C.1. Experimental Setting Details

Configuration: We developed a federated learning simulator to extensively evaluate the performance of various algorithms, models, datasets, and networks. We used TensorFlow 1.14.0 to implement federated learning⁴ and ns-3 3.30 to simulate the network on servers with Intel Core i7-6700 and NVIDIA TITAN X. For reproducibility, we provide the source code at <https://bit.ly/39g10Ip>.

Models: We used following *three* training models.

- The softmax regression (SR) involved 7,850 parameters.
- The 2 layered perceptron neural network (2NN) contained two hidden layers each with 200 units and ReLU activation; it contained 199,210 parameters.
- The convolutional neural network (CNN) contained two 5×5 convolutional layers with 64 channels, each followed by 2×2 max pooling and local response normalization. After the two convolutional layers, a fully-connected layer with 256 units and ReLU activation was added; the output layer with softmax activation was added. The CNN contained 369,098 parameters. For CelebA, the benchmark CNN, provided by Caldas et al. (2018), was used, and it contained 124,808 parameters.

Metrics: We evaluated the performance of the algorithms using the following metrics. The *test accuracy* was mea-

⁴TensorFlow Federated (Google, 2019) does not fully support the parallelism level of this simulation yet.

Table 4: Summary of parameters (the default value in bold).

Category	Parameter	Value
Model	Batch size	32, 64, 128 , 256, 512
	Learning rate	$10^{-3}, \dots, \mathbf{10^{-1}}, \dots, 10^3$
	Learning rate decay	0.99
Algorithm	Learning steps	$\tau = 5, \tau_1 = 1, \tau_2 = 5$
	# of groups	2, 5 , 10, 15, 20, 30

sured to evaluate the training progress and the predictive accuracy, respectively. In addition, the *epoch* and the *time* taken to reach a target test accuracy were measured to evaluate the convergence speed.

Hyperparameters: Table 4 lists the hyperparameters used for the model and the algorithm.

- **Model:** We searched the best batch size and learning rate for each model as follows. For the SR, 2NN and CNN models, the batch size was varied from 32 to 512 with an increment rate of 2, and the learning rate (η) was varied from 10^{-3} to 10^3 with an increment rate of 10. For the CNN model used for the CelebA dataset, the batch size was set to 5, and the learning rate was set to 0.001, as suggested by Caldas et al. (2018).
- **Algorithm:** FedAvg takes a single learning step (τ) as its input, whereas HierFAVG and FedAvg-IC take two learning steps (τ_1 and τ_2). To solely focus on the effects of communication, the product of all the learning steps of each algorithm was determined to be 5, which was one of the suggested values by McMahan et al. (2017). In FedAvg-IC, the number of groups $|\mathcal{K}|$ was varied in the range of $[2, 5, 10, 15, 20, 30]^5$. We also note that, in Algorithm 1, the K-MEDOID_GROUPING was performed only once at the beginning (Line 14), and the number of maximum steady steps was set to 1 (Line 19), which exhibited sufficiently high accuracy for the most of experiments despite the decreased optimization opportunities.
- **Environment:** We determined the default environment parameters by adopting commonly used ones in the previous studies (McMahan et al., 2017; Liu et al., 2019; Wang et al., 2019; Caldas et al., 2018).

In addition, to incorporate the unbalanced property (McMahan et al., 2017), the number of classes per node or edge and the number of data examples per node were randomly sampled from the normal distribution.

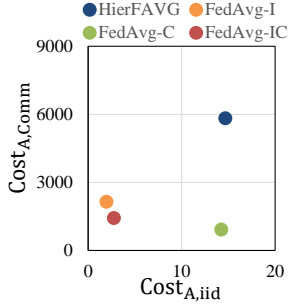


Figure 6: Cost analysis of the CNN on MNIST-F.

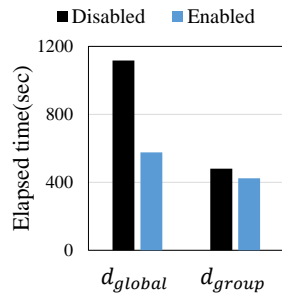


Figure 7: Effect of the combined aggregation.

C.2. Evaluation Details

The higher accuracy of FedAvg-IC in Section 6.2 is attributed to a decreased Δ in the IID cost in Eq. (12). As shown in Fig. 6 for the CNN on MNIST-F (Fig. 3b) with the Dtt setting, FedAvg-IC significantly decreased the $COST_{A,iid}$ that models Δ . This conforms to Remark 1.

The faster convergence speed of FedAvg-IC in Section 6.3 is attributed to a decreased d_{group} in Eq. (12) as well as a decreased communication data size by the combined aggregation. As shown in Fig. 6, FedAvg-IC significantly decreased the $COST_{A,comm}$ that models d_{group} . This is consistent with Remark 2. It should be also noted that FedAvg-IC finds a set of Pareto optimal solutions in Fig. 6 whereas HierFAVG exhibits non-optimized costs. Furthermore, as shown in Fig. 7, the communication time—especially, for the global aggregation—dropped rapidly when the combined aggregation was enabled.

C.3. Additional Results

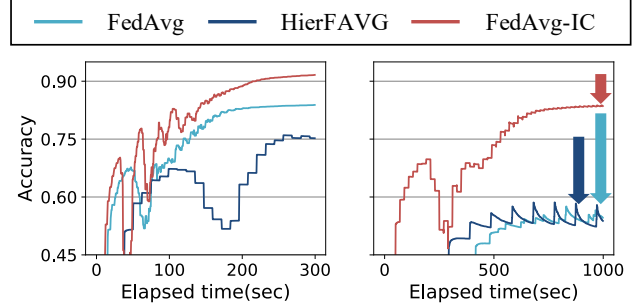
C.3.1. EFFECTS OF DIFFERENT SIMULATION SETTINGS

Effects of Computation Settings: We compared different processing speeds (5^6 and 250^7 GFLOPS). As shown in Fig. 9, the results with a high processing speed (Fig. 9b and 9d) exhibited higher accuracy than the ones with a low processing speed (Fig. 9a and 9c), which is attributed to the increased number of epochs. Furthermore, we investigated the effects of different learning steps. As shown in Fig. 8, the results with a small number of steps (Fig. 8a) exhibited higher accuracy than the ones with a large number of

⁵A sophisticated heuristic for determining the number of groups is an important issue in group federated learning, and we leave it as future work.

⁶This value is the average speed of Exynos 8895 in Samsung Galaxy S8. See <https://www.anandtech.com/show/11540/samsung-galaxy-s8-exynos-versus-snapdragon/2>.

⁷This value is the average speed of PowerVR GT7600, the most widely-used smartphone GPU in 2019. See <https://deviceatlas.com/blog/most-used-smartphone-gpu>.



(a) A small number of steps ($\tau = 5$ & $(\tau_1, \tau_2) = (1, 5)$). (b) A large number of steps ($\tau = 25$ & $(\tau_1, \tau_2) = (5, 5)$).

Figure 8: Effects of learning steps for the CNN on MNIST-O (Dtt).

steps (Fig. 8b), because the convergence upper bound became larger with a larger number of learning steps according to Theorem 1. It should be also noted that FedAvg-IC exhibited the lowest accuracy degradation, as indicated by the arrows in Fig. 8b; from Remark 1, when Δ is sufficiently minimized, other parameters hardly influence the convergence upper bound.

Effects of Communication Settings: We compared different network types (fat tree and jellyfish) and link speeds (10 and 100 MBps⁸). As shown in Fig. 9, the results with the jellyfish (dashed lines) converged faster than the ones with the fat tree (solid lines), which is attributed to the increased throughput of the cost-efficient jellyfish network (Singla et al., 2012). In addition, the results with a high link speed (Fig. 9c and 9d) converged faster than the ones with a low link speed (Fig. 9a and 9b), as marked by small circles in the figures with a high link speed that represent the time taken to train the same number of epochs as with a low link speed.

Effects of Data Distributions: Fig. 10 shows the accuracy results for different data distributions. As the variance of a distribution became higher (Fig. 10c and 10d), the learning curves for all algorithms became noisier. Nevertheless, FedAvg-IC still converged the fastest even with the noisier curves. We note that the mean of each data distribution does not need to be varied because, from the explanation of the data distribution in Section 6.1, it was determined to be the number of classes or data examples per node.

C.3.2. EFFECTS OF THE DEGREE OF NON-IIDNESS

Fig. 11 shows the effects of class diversity (i.e., non-IIDness). In all cases, FedAvg-IC outperformed the state-

⁸These values represent the state-of-the-art mobile connection speeds (Cisco, 2020).

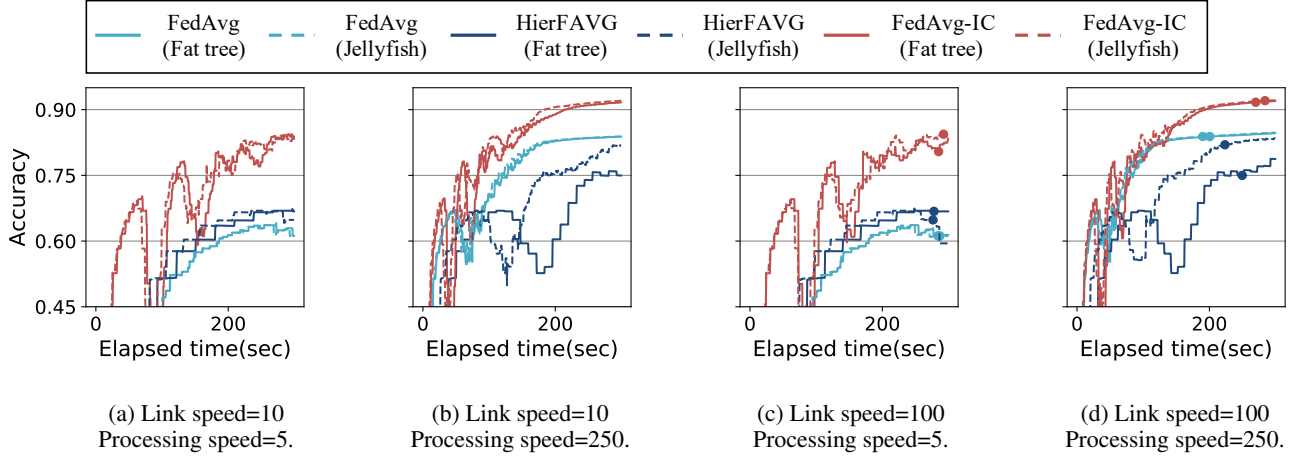


Figure 9: Effects of different communication and computation settings for the CNN on MNIST-O (D_{tt}). The standard deviation is not represented here to clearly convey the differences.

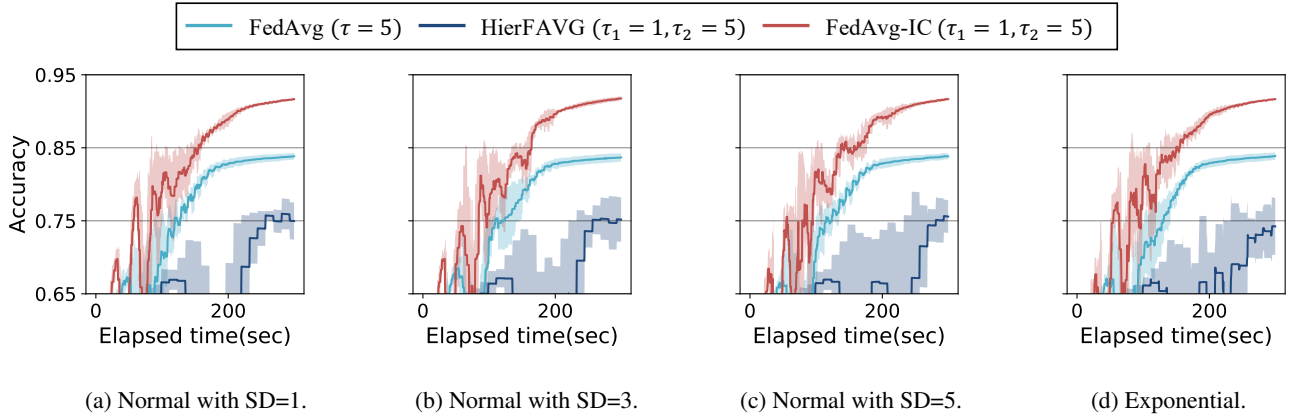


Figure 10: Effects of data distributions for the CNN on MNIST-O (D_{tt}).

of-the-art algorithms. When the data distribution in a node is non-IID (i.e., D_{tt} , D_{tq} , and D_{th}), FedAvg that is a node-based learning did not work well. In contrast, when the data distribution in an edge is non-IID (i.e., D_{tt} , D_{tq} , and D_{qq}), HierFAVG that is an edge-based learning did not work well. It should be noted that, because a node or an edge is very unlikely to be perfectly IID, the superiority of FedAvg-IC over the others will be valid in the real-world scenarios. Further evaluation with more realistic data distribution remains as future work.

Fig. 12, Fig. 13, and Fig. 14 show the accuracy results on MNIST-F, FEMNIST, and CelebA, respectively. The overall trends are shown to be similar to Fig. 11. The learning curves are represented with the elapsed time in the subfigures (a)–(c) and with the number of epochs in the subfigures (d)–(f). The results with the D_{qq} , D_{qh} , and D_{hh} settings are omitted because all curves closely overlap as before.

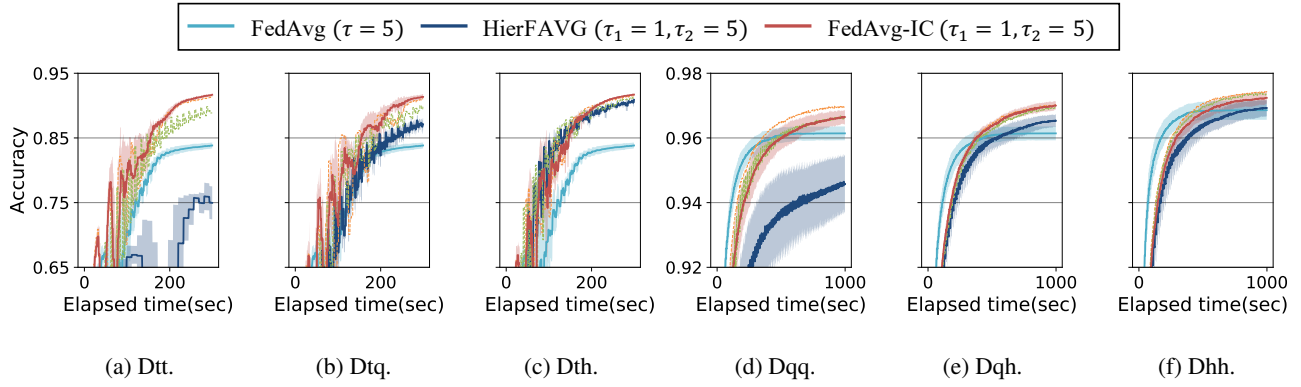


Figure 11: Effects of class diversity for the CNN on MNIST-O (Fig. 3a): Dtt Non-IID \longleftrightarrow IID Dhh .

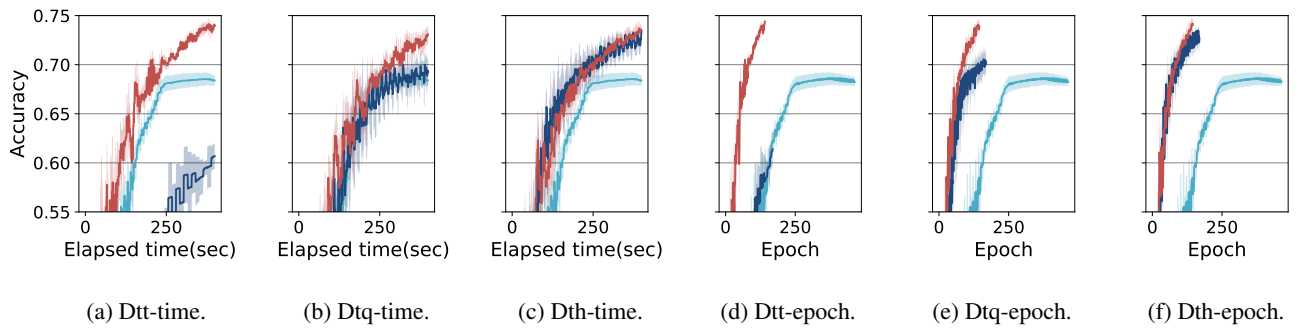


Figure 12: Effects of class diversity for the CNN on MNIST-F: Dtt Non-IID \longleftrightarrow IID Dth .

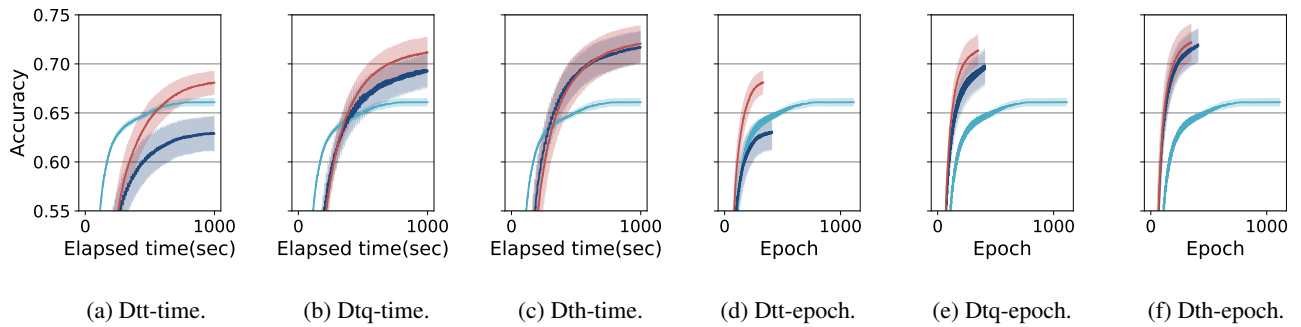


Figure 13: Effects of class diversity for the CNN on FEMNIST: Dtt Non-IID \longleftrightarrow IID Dth .

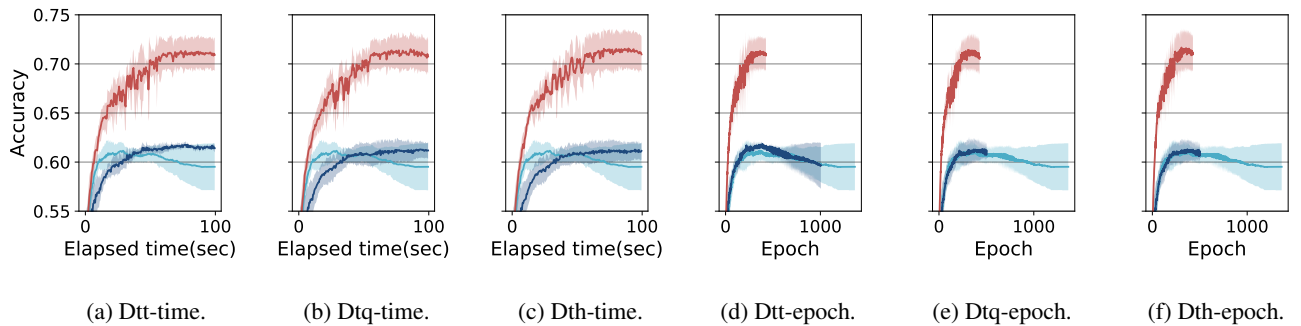


Figure 14: Effects of class diversity for the CNN on CelebA: Dtt Non-IID \longleftrightarrow IID Dth .